SURFACE CRACKING CAUSED BY ELECTROMAGNETIC WAVE ABSORPTION

BY

R.C.GOOD JR.

GENERAL ELECTRIC COMPANY

VALLEY FORGE SPACE TECHNOLOGY CENTER

BOX 8555,PHILA 1, PA.

FOR

CONTRACT NO. A F 49-638-1030

TASK NO. 37718, PROJECT NO. 9782

DIRECTOR OF AEROSPACE SCIENCES

AIR FORCE OFFICE OF SCIENTIFIC RESEARCH

WASHINGTON 25, D.C.

Surface Cracking Caused by Electromagnetic Wave Absorption

by

Robert C. Good, Jr.

Space Sciences Laboratory

Valley Forge Space Technology Center

General Electric Company

Contract No. AF 49(638)-1030
Task No. 37718, Project No. 9782
Director of Aerospace Sciences
Air Force Office of Scientific Research
Washington 25, D.C.

FOREWORD

The work reported here was done under a government contract with the Air Force Office of Scientific Research. The contract number was AF 49(638)-1030 as Task No. 37718, Project No. 9782, and the contract ran from March 1961 through February 1962.

ABSTRACT

An Exploding Wire Facility has been used to irradiate glass disks to determine any damaging effects. At power levels of 10^7 watts deposited in the wire, the glass surface has become crazed to a depth of 10^{-3} cm. Photo-micrographs and profilometer measurements of the surface are presented to support the following conjectures as to the cause of cracking: the energy radiated by the hot wire is absorbed by a thin surface layer of the glass, the temperature rises creating thermal stresses, flaws below the glass surface form stress raisers according to the Griffith crack theory, and the cracks propagate to the surface. The theoretical derivation of the adapted thermoelastic stress theory predicts the dimensions of the cracks and the power levels required if the absorption coefficient is at least 10^3 reciprocal centimeters.

TABLE OF CONTENTS

LIST OF ILLUSTRATIONS

I. INTRODUCTION

Studies of radiation damage are conducted by exposing samples to high intensity sources. History has carried accounts of many types of irradiation experiments. Simple exposure to the Sun's rays convinced man that he needed a concentrated source, and his use of chemical flames convinced him that he needed a high temperature source. Thus, man has sought concentrated, hot sources that last as long as possible. However, since intense radiations are emitted by sources operating at high power levels, man-made sources being relatively weak can be improved by pulse operation[1,6]. Explosions were the order of the day. Chemical explosives yield high power levels, but the attendant shock waves cloud the radiation effects. Electrical explosions such as arcs or sparks radiate more of their energy as electromagnetic waves than do chemical explosions[2]. Further, if the sources are placed in a vacuum, the shock waves are repressed so that sample damage can be correlated with radiation alone.

Many laboratories have designed and built different types of radiation sources. The Space Sciences Laboratory has built an exploding wire facility to irradiate various materials with electromagnetic waves. The wire is exploded by passing huge currents through it so that a hot plasma of metal particles radiates electromagnetic waves. The power level of the source has been raised to the point at which damage can be inflicted in glass, china and textolite. The general level is 3000 joules discharged in ten microseconds or 3×10^8 watts.

The tests to be described below were made by exposing glass samples, which formed part of an evacuated chamber, to the radiations from an exploding wire. The following events were postulated to occur: (1) Energy stored in a capacitor bank was deposited in a two-mil wire so rapidly that it heated to an incandescent plasma, (2) The hot plasma radiated energy throughout the electromagnetic spectrum, (3) Waves of all frequencies traveled essentially unimpeded through the chamber to the sample, (4) The glass transmitted some frequencies and absorbed others by conversion to heat, (5) Absorption occurred very close to the surface for waves in the ultra-violet region since the glass cut-off characteristic is sharp,

(6) Thermoelastic stresses were set up in the glass, (7) The free surface of the glass cracked since the glass was frangible and the heating period was too short to permit stress equalization, (8) The surface melted if the power level were high enough, and then, (9) The surface cooled without destroying the original crack pattern.

II. THEORETICAL DERIVATION OF THERMOELASTIC STRESSES

To set a proper background for our explanation of the damage in the glass samples, the appropriate theories should be invoked to derive the necessary relations. Proceeding through the events listed before, we will discuss the conversion of electrical energy to heat in the wire, the radiation of electromagnetic waves, the absorption of the waves, the production of the thermal stresses, and the cracking processes.

A. Conversion of Electrical Energy to heat in the wire.

This subject has been covered by others[3, 5]. Suffice it to say here that the main problem is time. Pulses must be short enough to deposit energy in the wire, and its heated products, before it flies apart. Low inductance in the electrical circuit keeps the pulse short, low resistance decreases the power losses, and impedance matching provides adequate power transfer.[4]

B. Radiation of Electromagnetic Waves.

Normally, the wire material radiates as a black body in a continuous spectrum. Also, it emits its characteristic spectrum in which the line intensities depend upon the properties of the atoms and the temperature of the plasma. As will be seen later, we are particularly interested in the short wave-lengths. If black body radiation is prevalent, the proportion of energy radiated in the ultraviolet is greater if the temperature is higher. If spectral radiation is prevalent, ultraviolet light will be emitted only if the atoms are excited to higher energy states. Thus, high temperature plasmas are needed in both cases.[1, 6]

Again we state that these are not new principles and will not be discussed further here. An important consideration is that the geometry of the system should be designed so the waves are essentially plane waves when passing through the sample.

C. Absorption of Electromagnetic Waves.

As electromagnetic waves pass through glass, the amount of energy that is absorbed depends upon the conductivity of the glass.[13]

Solutions of Maxwell equations for plane waves in an unbounded medium indicate that the conductivity is included in the complex propagation constant. When using this constant in calculating the Poynting vector

$$\bar{S} = \frac{1}{2} \bar{E} \times \bar{H}^* \tag{1}$$

we find that a dissipative term appears. ($\bar{E}$ is the electric field vector and $\bar{H}^*$ is the complex conjugate of the magnetic field vector). According to Poynting's theorem the divergence of $\bar{S}$ measures the energy transformed per unit volume per second into heat. Thus, for plane waves

$$\bar{E} = \bar{E}_o \exp\left[-\frac{bx}{2} + i\alpha x - i\omega t + \theta\right] \tag{2}$$

and

$$\bar{H} = \bar{H}_o \exp\left[-\frac{bx}{2} + i\alpha x - i\omega t\right] \tag{3}$$

where the wave is propagating in the positive x direction, $\frac{b}{2}$ is the complex part and α the real part of the propagation constant, ω is 2π times the frequency, t is the time, θ is a phase constant, and $\bar{E}_o$ and $\bar{H}_o$ are the maximum magnitudes of the field. The value of $\bar{S}$ is

$$\bar{S} = \frac{1}{2} \bar{E}_o \times \bar{H}_o e^{-bx + \bar{\theta}} \tag{4}$$

and the divergence is

$$\nabla \cdot \bar{S} = -\frac{ab}{\mu\omega} |E_o|^2 e^{-bx} \tag{5}$$

where μ is the permeability of the glass. In terms of the conductivity σ and permittivity ϵ, we find

$$\nabla \cdot \bar{S} = -\frac{\sigma}{2} |E_o|^2 \exp(-\sigma x \sqrt{\mu/\epsilon}) \tag{6}$$

The divergence of the Poynting vector measures the energy transformed per unit volume per second into heat.

The important feature of this expression is that the amount of energy converted to heat within the glass is an exponential function of the distance from its surface.

D. Production of Thermal Stresses.

D. (1) Derivation of Temperature as a Function of Time and Distance

A pulse of electromagnetic waves produced by the exploding wire enters and is absorbed by the glass thus forming internal heat sources. A thermal spike is created and propagated as a spike because the thermal diffusivity is small. This sequence can be expressed in the thermal diffusion equation which contains a heat-conduction term, a heat-sink term, and a heat-generation term.[16] The equation is

$$(7) \qquad K(\partial^2 T/\partial x^2) - c\rho\,(\partial T/\partial t) + A_o \exp(-bx) = 0$$

in which K is the thermal conductivity, T is the temperature rise, x is the distance from the surface into the glass, c the specific heat of the glass, ρ the glass density, t the time, A_o the rate of conversion of electromagnetic energy into heat and b is the coefficient of absorption.

We note from equations (6) and (7) that

$$(8) \qquad A_o = \frac{\sigma}{2} |\bar{E}_o|^2$$

which is a constant if $\bar{E}_o$ is a constant. In the pulse of electromagnetic energy, $\bar{E}_o$ is a function of time and wave-length; however, in lieu of further measurements* we have taken the pulse to be square for this analysis. Thus A_o is constant during the pulse and zero thereafter. Since the glass temperature reaches a maximum when the electromagnetic waves stop, the equations have been solved only for times during the pulse.

* Light probe measurements shown in Figure 7 indicate a fairly well defined pulse that could be averaged out to a square pulse.

The boundary conditions for the differential equation have been chosen as follows: At zero time the glass is at the same temperature as the surroundings, and at the surface the glass radiates energy proportional to its temperature rise above the surroundings. This is an approximation of the Stefan-Bolzmann radiation law justified only if the temperature rise is small. Radiation from the hot plasma is assumed to be completely accounted for by the A_o term. Convection currents and conduction effects are minimized by the low pressure maintained in the chamber. Thus:

(9) $\quad$ at $t = 0$; $\quad T = 0$

(10) $\quad$ and at $x = 0$; $\quad K\partial T/\partial x = HT$

where H is the energy transfer coefficient of the glass surface. The solution is expressed in terms of error functions defined by

(11) $$\operatorname{erf}(z) = (2/\sqrt{\pi}) \int_0^z \exp(-z^2)\, dz.$$

By combining solutions of thermal diffusion equations on pages 70 and 78 of reference 14, we find the solution to equation (7) to be

(12)
$$T(x,t) = (A_o/K) \left\{ \left[(H + bK)/b^2H\right] \left[1 - \operatorname{erf}(x/2\sqrt{Kt/c\rho})\right] - (1/b^2)\exp(-bx) \right.$$
$$+ (1/2b^2) \exp(-bx + Kb^2 t/c\rho) \left[1 + \operatorname{erf} \frac{x - 2Kbt/c\rho}{2\sqrt{Kt/c\rho}}\right]$$
$$- \left[(H+Kb)/2b^2(H - Kb)\right] \exp(bx + Kb^2 t/c\rho) \left[1 - \operatorname{erf} \frac{x+2Kbt/c\rho}{2\sqrt{Kt/c\rho}}\right]$$
$$\left. + \left[K^2/H(H - Kb)\right] \exp(Hx/K + H^2 t/c\rho K) \left[1 - \operatorname{erf} \frac{x+Ht/c\rho}{2\sqrt{Kt/c\rho}}\right] \right\}$$

The values for K, c, and ρ do not vary greatly for different glasses. H can be found from the Stephan Bolzmann relation for black body radiation.

This equation may be used to compute the temperature at any time and at any point in the glass. Of course, T can be obtained only if b and A_o are assumed; therefore, theory can be matched with experiment by determining the values of b and A_o which produce the best fit.

We have limited t to the pulse length (ten microseconds) and x to the distance (ten microns) of the cracked region in the glass. Approximating the exponential function by a series expansion is convenient since the arguments are small. Also if $Kt/c\rho$ is much smaller than x/b and Kx/H the expression for the temperature may be approximated by the equation

$$(13) \qquad T(x, t) = A_o \left[(H + bK)/6K^2\right] \left[1 - \text{erf}(x/2\sqrt{Kt/c\rho})\right] x^3$$

Figure 1 shows the results of computations using this approximation. A thermal spike travels through the glass slowly during the absorption process. Only the first ten microseconds are shown because the radiant pulse lasts only that long. Thereafter, the temperature can only decrease as the heat dissipates throughout the disk.

For larger values of b the approximation for $T(x, t)$ has additional terms. Since the $\text{erf}\, z$ is almost linear in the region in question, the function can be expanded in a Taylor's Series. Thus,

$$(14) \qquad \text{erf}(z + \delta) = \text{erf}\, z + \frac{2}{\sqrt{\pi}} \delta e^{-z^2} + \ldots$$

in which δ contains the term in b. When this is used, the approximate solution for $T(x, t)$ becomes

$$T(x,t) = \frac{A_o}{b^2K}\left\{\left[(II + bK) / 6K\right] \left[1 - \mathrm{erf}(x/2\sqrt{Kt/c\rho})\right] x^3 b^2\right.$$

$$- \left[1 - \exp(Kb^2t/c\rho)\right] \exp(-bx)$$

$$- \left[\cosh bx + (II/bK) \sinh bx\right] \left[2b\sqrt{Kt/c\rho\pi} \exp(-x^2c\rho/4Kt) \exp(Kb^2t/c\rho)\right]$$

$$\left. - \left[(II/bK) \cosh bx + \sinh bx\right] \left[1 - \exp(Kb^2t/c\rho)\right]\left[1 - \mathrm{erf}(x/2\sqrt{Kt/c\rho})\right]\right\}$$

(15)

Figure 2 shows the calculated values using this approximation. The thermal spike travels through the glass just as on Figure 1. However, the ordinates are about 10^4 times larger which indicates that more heat is being deposited in the glass.

D. (2) Derivation of Quasistatic Thermoelastic Stresses.

The temperature distribution derived above is a planar distribution; therefore, in a semi-infinite body all stresses and strains will be constant over planes parallel to the surface. Furthermore, the stress in the x direction (into the body from the surface) will be zero because that stress at the surface must be zero. Since the strain parallel to the surface must be zero, we have

$$\epsilon_y = \epsilon_z = 0 = \alpha T + \frac{1}{E}(\sigma_y - \nu\sigma_z) \tag{16}$$

and the stress parallel to the surface will be

$$\sigma_y = \sigma_z = -\frac{E\,\alpha\,T(x)}{1-\nu} \tag{17}$$

in which α is the coefficient of expansion, E is Young's modulus, and ν is Poisson's ratio.

E. Cracking Process.

The above reasoning has shown that compressive stresses in the glass are parallel to the surface. Also the stresses vary with distance beneath the surface and reach a maximum at a point about 10^{-4} cm from the surface (see figure 1). If the compressive stresses are large and are non-uniformly distributed, an instability is produced that can be alleviated by displacements at inherent imperfections or cracks.

A well known fact is that glass contains many flaws which act as stress raisers. Several relations between flaw geometry and stress concentration have been studied,[7-9] but the most generally accepted is that given by Griffith.[10] He predicts that the critical tensile stress for crack propagation is

$$\sigma_{cr} = \sqrt{4E\Sigma/\pi w} \tag{18}$$

where Σ is the surface energy and w is the crack width.

Since thermal stresses are compressive, the Griffith relation is not strictly applicable. However, the following explanation is offered to show that tensile stresses may be found at the ends of elliptical flaws. Figure 3a shows a flaw oriented so that σ_y acts along its major axis and σ_z acts perpendicular to the plane of the paper. In this case the stresses at the points A and A^1 may be calculated from two dimensional theory. Timeshenko[11] shows that the stress at $A - A^1$ is equal in magnitude and opposite in sign to σ_y. (Because the theory is linear, the same expression applies to compressive stresses). Thus at the points $A - A^1$ there can be three stresses: σ_y, σ_z, and $-\sigma_y$ in the x direction. If we use the maximum difference in stress criterion for fracture, the addition of σ_z does not affect the result since $\sigma_z = \sigma_y$. Nevertheless, σ_{cr} in equation 16 is given by $-\sigma_y$, because σ_{cr} is a tensile strength having little to do with yield stresses.[7]

By combining equations 6, 8, and 4 (which may be written as

$$S = \frac{1}{2} E_o^2 \sqrt{\frac{\epsilon_a}{\mu_a}} \tag{19}$$

where the subscript "a" refers to the air in front of the glass), we find that

$$S = A_o/(\phi \sqrt{K_g}) \tag{20}$$

in which K_g is the dielectric constant of the glass. Let us assume that the σ_z in equation 17 is that given as σ_{cr} in equation 18. Further, let the ordinates (TK/A_o) be called q. In that case

$$S = \sigma_z (1 - \nu) K/E\, a\, qb \sqrt{K_g} \tag{21}$$

in which σ_z, ν, K, E, a, and K_g are constants so that

$$S = \frac{G}{qb} \tag{22}$$

The cracks are produced parallel to the surface as shown if equation 16 is satisfied. At flaws which are oriented at a small angle ϕ, the stresses are shown in Figure 3b and the cracks will propagate toward the surface. These assumptions indicate a process for the formation of surface cracks: (1) the temperature is raised in the material close to the surface producing thermal stresses, (2) the critical stress for crack propagation is attained, and (3) the crack width is larger than the distance to the surface from the flaw.

III. EXPERIMENTAL APPARATUS AND PROCEDURES

An exploding wire facility has been built at the Space Sciences Laboratory. A schematic diagram is shown in Figure 3. A high voltage power supply is used to charge two capacitor banks in series with the explodable wire between them. When charged, the high voltage terminal is shorted to ground, thereby completing the circuit through the wire. A voltage divider on the low voltage side of the wire provides a signal for triggering the oscilloscopes and for wave analyses.

Twelve low-inductance type K clamshell inductances are charged to 80KVDC (40KV across each bank) in order to store 9600 joules. The ringing frequency is 300KC and there are 4 cycles in each pulse that indicate substantial power. With a pulse lasting about 10 microseconds the rate of energy dissipation would be about 10^9 watts.

Circuit inductance is minimized by using wide flat copper plates for the busbars, by using a specially designed feed for the wire, and by using a shorting switch of coaxial design. Two layers of thin Mylar sheet (0.015") separate the plates and maintain the high electrical field.

The shorting switch is a Jennings Manufacturing Company vacuum switch that is mechanically activated by a solenoid. Tungsten electrodes form the spark gap which may be adjusted for varying voltages.

The exploding wire load is contained in the central segment of the mirror facility and represents the common focus of the two intersecting ellipsoids. A close-up view of this cartridge is shown in Figure 5. The cartridge is open on both ends and includes part of the ellipsoidal mirror such that the acceptance angle of the individual mirror on either side is almost 180°. The cartridge is made so that it may be closed by placing glass windows on either side in place of the ellipsoids. Electrodes are introduced into the chamber from both sides and are adjustable for a gap of one to two centimeters. A two mil tungsten wire connects the electrodes and forms the plasma that supports the spark.

Each of the two symmetrically arranged ellipsoidal mirrors is made in two halves that are bolted together at the plane of the minor axis. Individual halves were shaped from pyrex tubes collapsed over an ellipsoidal steel mandrel, polished to 25 Angstroms surface finish. The glass was coated with a film of platinum for adequate reflection of the short wave length waves. End caps enclose the second focus of the ellipsoids at which samples may be placed.

One side of the cartridge provides a vacuum port and a focus for spectroscopic measurements. At the other side specimens are irradiated at the focal point of the mirror. The glass samples are 3/4 inch in diameter and any thickness up to 1/2". The pressure in the system is maintained at 10^{-5} mm of Hg. At this pressure the mean-free-path is five centimeters, the density is low enough to prevent excessive attenuation of short waves, and shock waves are restricted.

A typical spectrum taken with a Bausch and Lomb grating spectrograph is shown in Figure 6. Although this was taken at a power level of 900 joules, the profuse lines of tungsten are evident. Two lines of copper, 5105.5 and 5153.2A, were found from which a temperature of 6300°K was calculated. The copper lines were used in this calculation rather than the tungsten lines because their transition probabilities were known, whereas those for the tungsten lines were not known.

The light flash was measured with a 929 photocell set up to view the flash from six meters. A typical record is shown in Figure 7. The pulse had a rapid build up and a slow fade out during a ten microsecond period. Square waves of 20 to 500 KC from a General Radio oscillator were passed by the electrical circuit without distortion. Hence, the wave form of Figure 7 which has a base frequency of 100 KC may be regarded as a true reproduction.

Pyrex and lime glass disks were cleaned thoroughly and examined for flaws before exposure. They were placed in the cartridge or at the focus of the ellipsoidal mirrors. The damage which occurred on the exposed surface was measured with a stereoptical

microscope and a profilometer. A sample photomicrograph is shown in Figure 8. The longest cracks were several millimeters long and the shortest were less than 0.1 mm. Different samples exposed to different power levels showed cracks of various lengths and number.

IV. RESULTS

An equation for the temperature distribution within the glass has been derived theoretically with the assumption that heat is generated within the glass. Two parameters are prominent in the equation: A_o and b. Several values of b have been used to calculate the temperature distribution. (The value of A_o does not affect the distribution but only the magnitude of the temperature.) Figure 1 shows the distribution for an approximation to the equation in which b was set equal to 0.6 cm^{-1}. (Values of 0.1, 0.6, and 1.0 cm^{-1} have been used in order to show the gross effects. For this approximation to be valid $Kbt/c\rho$ must be small compared to x.) The figure shows a thermal spike that grows and travels through the glass. The maximum temperature is shown at $x = 6 \times 10^{-4}$ cm.

When b is large enough to invalidate the approximation, another equation must be used in computing the temperature. Computations for $b = 10^3$ cm^{-1} show that the thermal spike travels through the glass but has a higher temperature because the energy is absorbed more rapidly in the glass. However, the shape of the spike is roughly the same. In this case the maximum occurs at $x = 4 \times 10^{-4}$ cm.

The compressive stresses have the same distribution as that shown in Figure 1 because the stresses are directly proportional to the temperature. The cracks will propagate according to Griffith's criterion as expressed by equation 18 in which σ_{cr} is the tensile strength for glass, 5000 psi. By using the surface tension of glass at room temperature[8], 560 dynes/cm, the width of the crack, w, is found to be 4×10^{-3} cm. The cracks can propagate in various directions, as shown in Figure 2, so that they may meander before reaching the surface. Since a factor of four is not unreasonable, cracks will appear at the surface if the stress reaches 5000 psi at points less than 10^{-3} cm deep. From equation 15 the temperature rise needed to produce thermal stresses of 5000 psi is 50°C. Using these values, we find the constant G in equation 22 to be 0.050 cal/cm sec.

Comparison of calculations with test results is given by these considerations: Figure 8a, taken at an energy level of 400 joules,

is close to the minimum level for cracking to occur. With pulsed energy the temperature must reach 50°C (that needed to produce the critical stress) late in the pulse; thus the top curves of Figures 1 and 2 represent the critical temperature. The maximum temperature (and stress) occurs 6×10^{-4} and 4×10^{-4} cm respectively from the surface which is close enough for cracks 4×10^{-3} cm wide to reach the surface. Representative values are given in Table I for the samples shown in Figure 8a, b, c.

Figure 8b, taken at an energy level of 600 joules, presents a higher energy level. Since A_o is proportional to the energy level when the efficiency of energy transformation is constant, the critical stress can be produced at a lower ordinate. Therefore, the cracks should occur sooner and closer to the surface, and more cracks will appear because there is extra energy available within the ten microsecond pulse.

Figure 8c, taken at an energy level of 900 joules, shows more profuse cracking. As in 8b, A_o is increased and the critical value of q decreases. At this level, cracks can form earlier so that many cracks will be found. In both 8b and 8c the depth of crack initiation is well within the limit of crack propagation.

TABLE I

Calculations for Power Intensity

Sample	Power joules	b cm^{-1}	Time sec	q cm^2	x cm	S - at sample watts/cm^2	S - at source watts/cm^2
Fig. 8a	400	0.6	10^{-5}	2.6×10^{-12}	5.5×10^{-4}	1.1×10^{11}	1.3×10^{12}
	400	10^3	10^{-5}	8.8×10^{-8}	3.6×10^{-4}	2.0×10^{3}	2.4×10^{4}
Fig. 8b	600	0.6	8×10^{-6}	1.7×10^{-12}	4×10^{-4}	1.7×10^{11}	2.1×10^{12}
	600	10^3	8×10^{-6}	5.9×10^{-8}	2.3×10^{-4}	3.0×10^{3}	3.8×10^{4}
Fig. 8c	900	0.6	6×10^{-6}	1.1×10^{-12}	3×10^{-4}	2.5×10^{11}	3.1×10^{12}
	900	10^3	6×10^{-6}	3.9×10^{-8}	1.6×10^{-4}	4.5×10^{3}	5.7×10^{4}

We note from Table I that the values of $\bar{S}$ at the source for $b = 0.6$ are quite unreasonable. The values for $b = 10^3$ are much closer since a black body at a temperature of 10^4 °K radiates 5×10^4 watts/cm^2 for the whole spectrum of which only 15% could be absorbed by the glass. Thus, we can say that the absorption coefficient of glass is within an order of magnitude of $10^3 cm^{-1}$.

Figure 9 shows a soda lime glass surface that has broken into slivers sticking up out of the glass. The energy stored for this test was 900 joules. On Figure 10 the surface has not only cracked but has a bubbly appearance between the cracks. Because the energy stored was 1500 joules, the surface was irradiated with a higher flux so that the surface partially melted before the end of the pulse. When the glass cooled down, the surface chips were left in this arrangement.

A profilometer measurement, Figure 11, indicated that the depth of cracking of a sample such as shown in Figure 10 was 500×10^{-6} inches or 1.2×10^{-3} cm. This represents the thickness of chips removed from the cracked surface for the purpose of the depth measurement. This measurement agrees with the values shown on Figure 1 and calculated by Griffith's criterion.

Figure 12 is shown to indicate that the cracking phenomenon is truly thermal in cause. A silver ring was painted onto the surface before irradiation. The photograph was taken to show that the cracks stopped a short distance away from the silver. Thus the silver not only shielded the glass from the electromagnetic waves but also cooled the glass sufficiently to prevent thermal stresses from reaching the critical stress necessary to crack the glass.

V. CONCLUSIONS

Cracks occur on glass surfaces under intense radiation because of thermal heating. The glass absorbs electromagnetic waves according to Poynting's theorem which gives an exponential law for the heating sources within the glass. The maximum temperature occurs very close to the surface. Thermal stresses are proportional to the temperature and are large enough to cause cracks that form to propagate from the points at the maximum stress to the surface.

ACKNOWLEDGEMENT

The author wishes to thank Dr. J. Heyda and Dr. A. Garofalo for their help with the solutions of the equations, and Dr. T.D. Riney and Dr. F.W. Wendt for their enlightening discussions of the theory and test results. Mr. C. J. Dudzinski prepared the samples and operated the equipment during the tests.

BIBLIOGRAPHY

1. Vanyukov, M.P. and Mak, A.A., High Intensity Pulsed Light Sources, Sov. Phys. Uspekhi, Vol. 66 No. 1 (1958) 137.

2. Kvarkhtsava, I.F. et. al., Electrical Explosions of Metal Wires, Sov. Phys. JETP, Vol. 3, No. 1, August 1956.

3. David, E., Physikalische Vorgänge bei elektrischen Drahtexplosionen, Z.f. Phys., Vol. 150 (1958) s 162.

4. Lebedev, S.V., Explosion of a Metal by an Electric Current, Sov. Phys. JETP, Vol. 5, No. 2, Sept. 1957.

5. Anderson, J.A. and Smith, S., General Characteristics of Electrically Exploded Wires, Astrophys. J., Vol. 64 (1926) 295.

6. Conn, W.M., The Use of Exploding Wires as a Light Source of Very High Intensity and Short Duration, JOSA, Vol. 41, No. 7, (1951) 445.

7. Orowan, E., The Mechanism of Seismic Faulting, Symposium on Rock Deformation, Inst. Geophys., Univ. Cal., Los Angeles, Nov. 1956.

8. Charles, R.J., A Review of Glass Strength, Gen. Elec. Res. Lab. Report No. 60RL-2314M, Jan. 1960.

9. Anderson, O.L., The Griffith Criterion for Glass Fracture, Chapter 17, "Fracture" Overbach, ed. John Wiley & Sons, Technology Press MIT, 1959.

10. Griffith, A.A., Phil. Trans. Roy. Soc., A221, (1921) 163.

11. Timoshenko, S. and Goodier, J.N., "Theory of Elasticity", 2nd ed. McGraw-Hill Book Company, New York, 1951, pg. 201.

12. Kee, H., High Temperature Properties of Glass, Prod. Eng., Vol. 32, No. 39, Oct. 16, 1961, pg. 84.

13. Stratton, J.A., "Electromagnetic Theory", McGraw-Hill Book Company, New York, 1941, pg. 281.

14. Carslaw, H.S. and Jaeger, J.C., "Conduction of Heat in Solids", Oxford Clarendon Press, 1959, pg. 78.

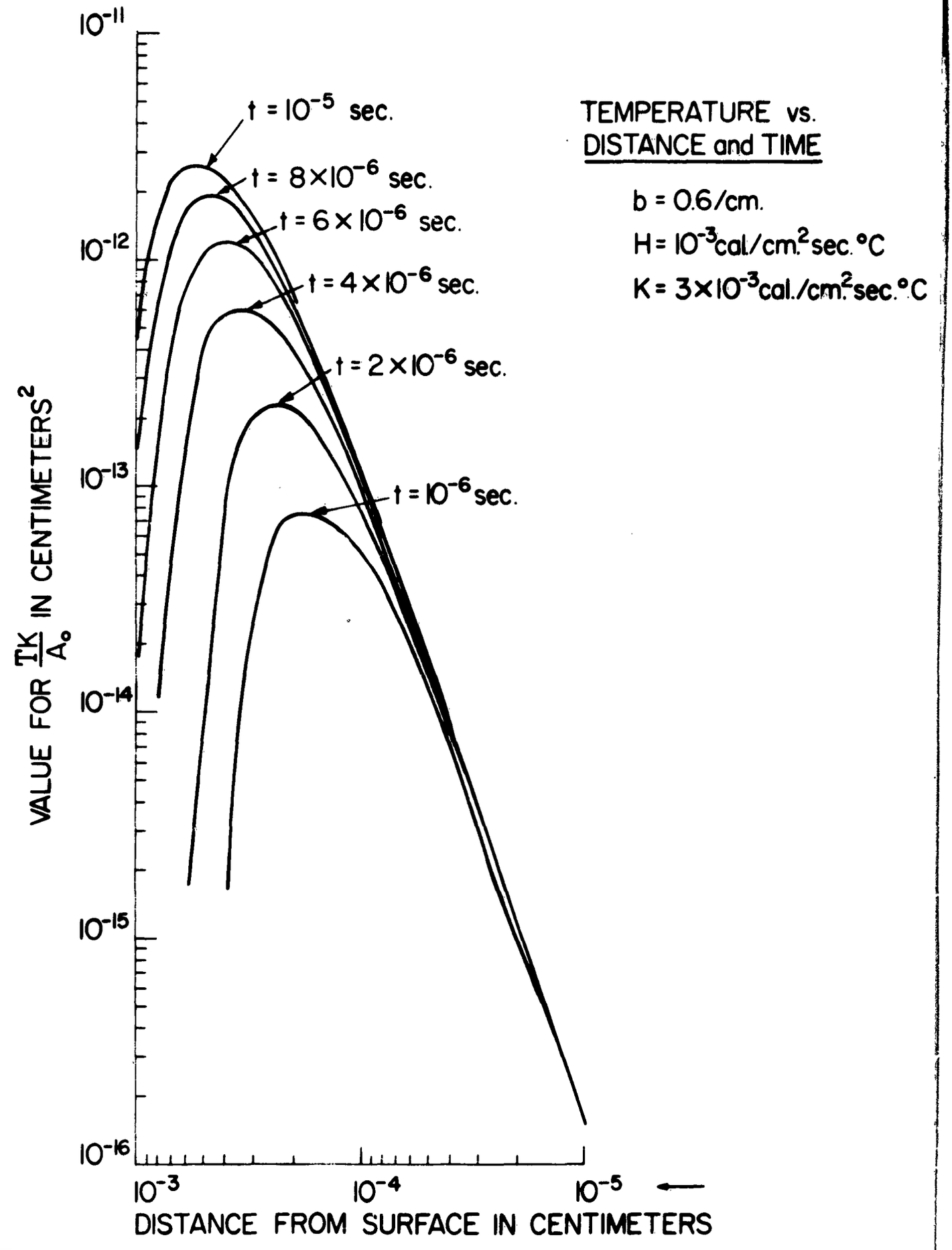
TEMPERATURE vs.
DISTANCE and TIME
b = 0.6/cm.
H = 10⁻³cal/cm.²sec.°C
K = 3×10⁻³cal./cm.²sec.°C
t = 10⁻⁵ sec.
t = 8×10⁻⁶ sec.
t = 6×10⁻⁶ sec.
t = 4×10⁻⁶ sec.
t = 2×10⁻⁶ sec.
t = 10⁻⁶sec.
VALUE FOR TK/A₀ IN CENTIMETERS²
10⁻¹¹
10⁻¹²
10⁻¹³
10⁻¹⁴
10⁻¹⁵
10⁻¹⁶
10⁻³
10⁻⁴
10⁻⁵
DISTANCE FROM SURFACE IN CENTIMETERS

Figure 1

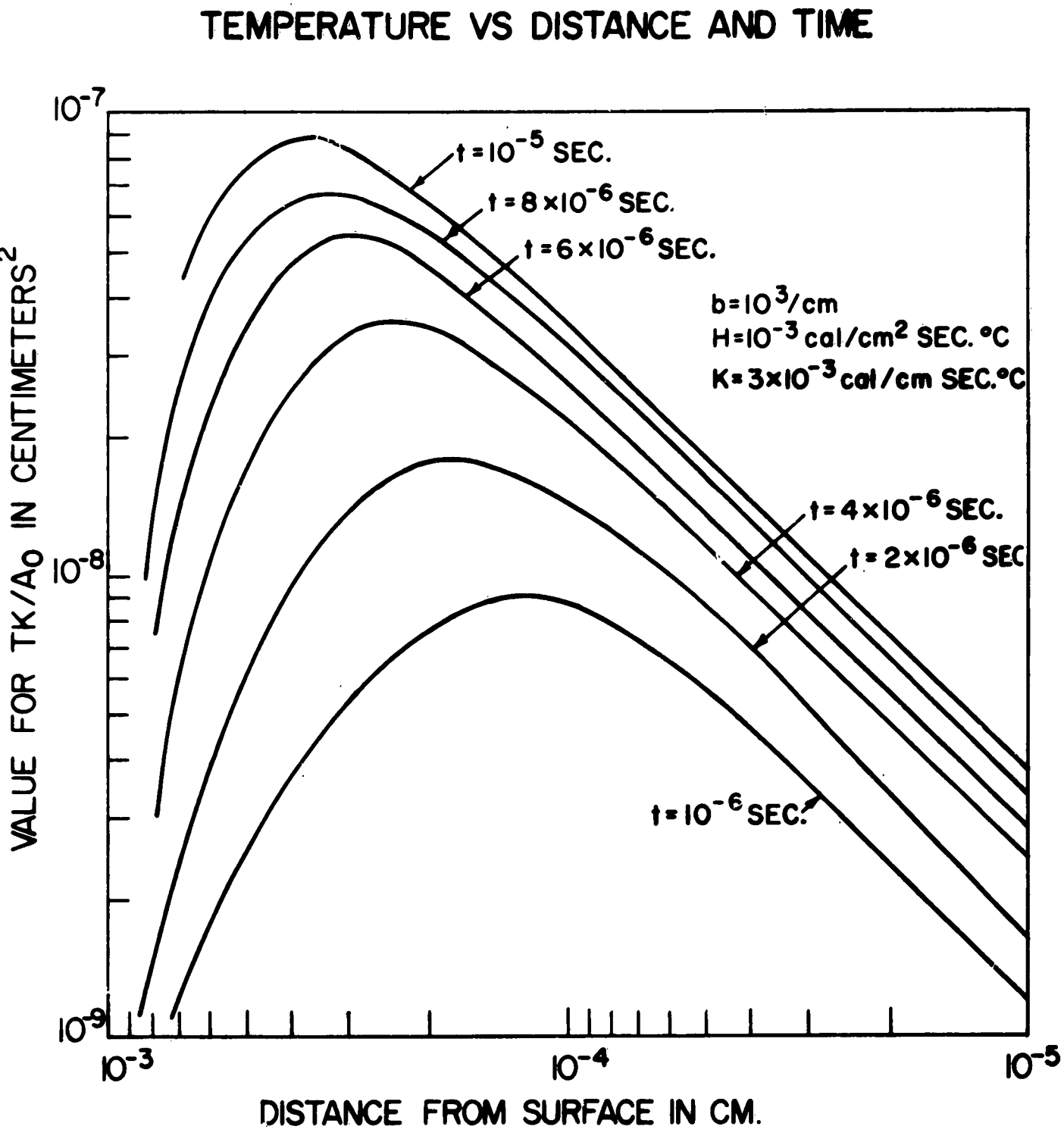
TEMPERATURE VS DISTANCE AND TIME
10^{-7}
10^{-8}
10^{-9}
VALUE FOR TK/A0 IN CENTIMETERS^2
t = 10^{-5} SEC.
t = 8×10^{-6} SEC.
t = 6×10^{-6} SEC.
b = 10^3/cm
H = 10^{-3} cal/cm^2 SEC. °C
K = 3×10^{-3} cal/cm SEC.°C
t = 4×10^{-6} SEC.
t = 2×10^{-6} SEC
t = 10^{-6} SEC.
10^{-3}
10^{-4}
10^{-5}
DISTANCE FROM SURFACE IN CM.

Figure 2

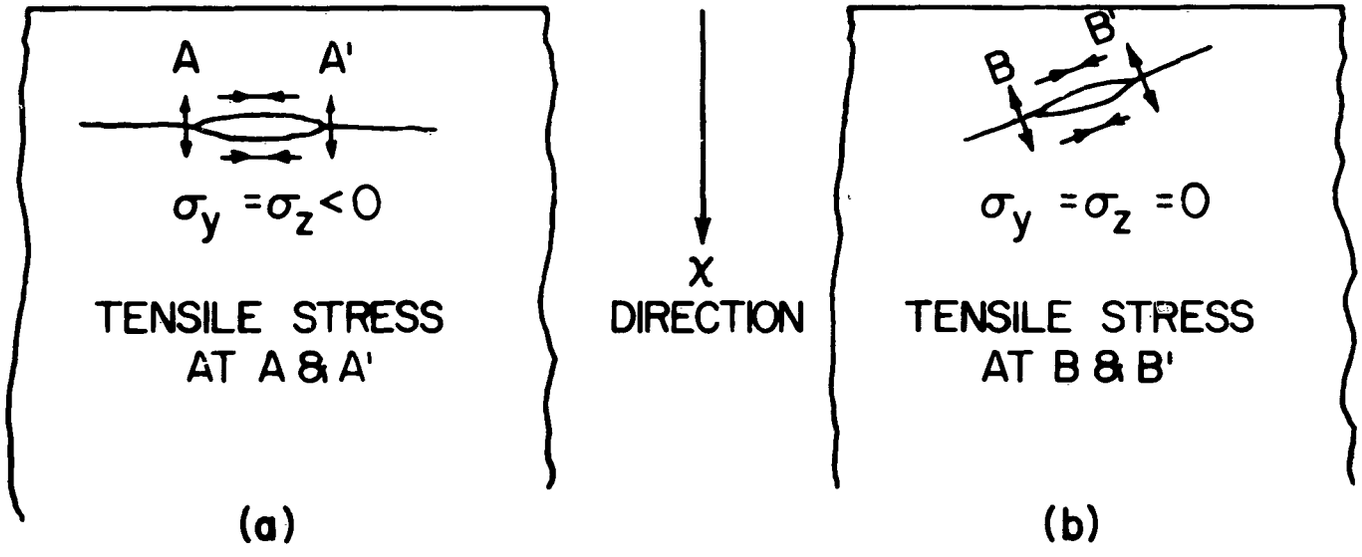

Figure 3. STRESSES AT ELLIPTICAL FLAWS IN A SEMI-INFINITE BODY

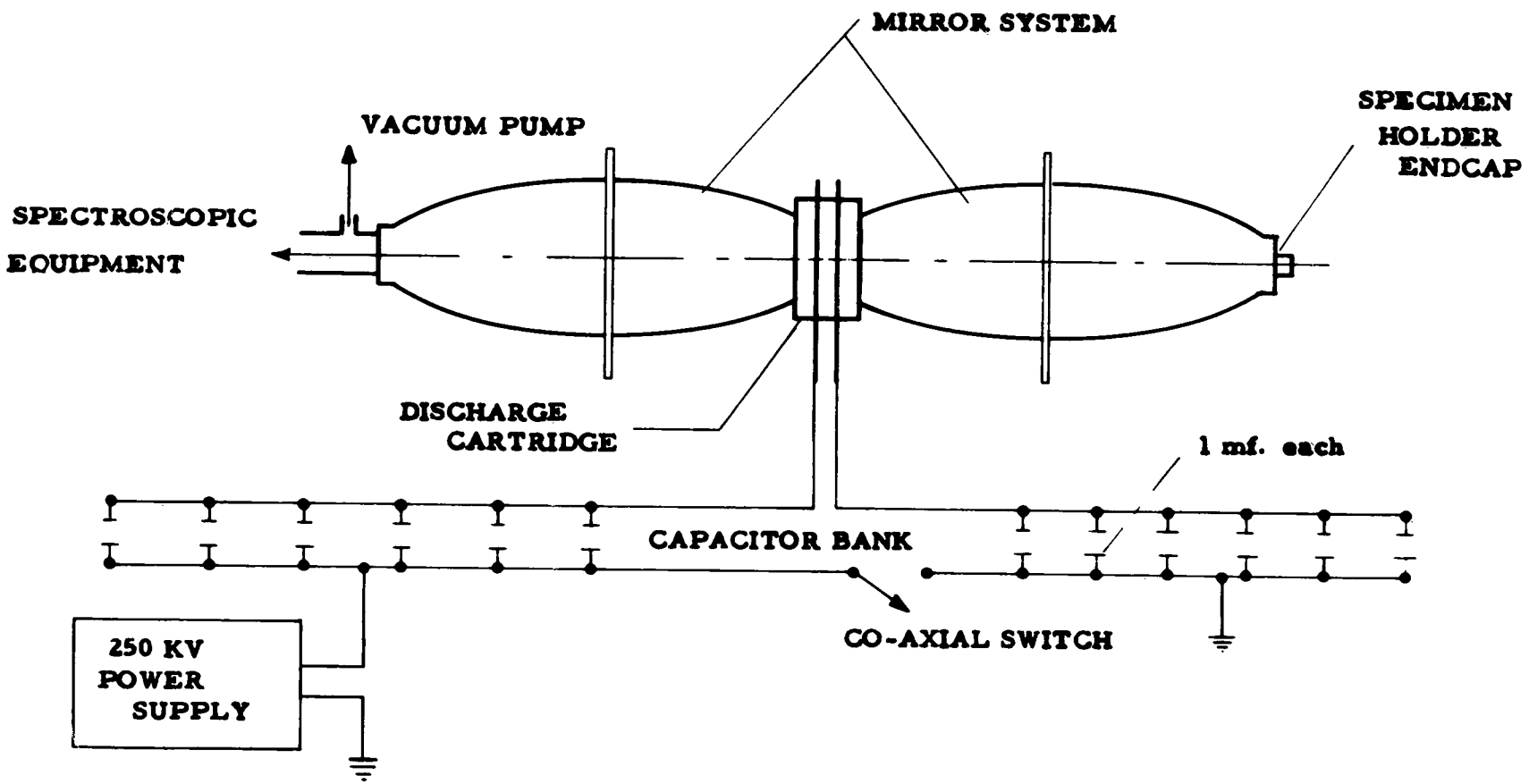

Figure 4. Schematic Arrangement of Facility

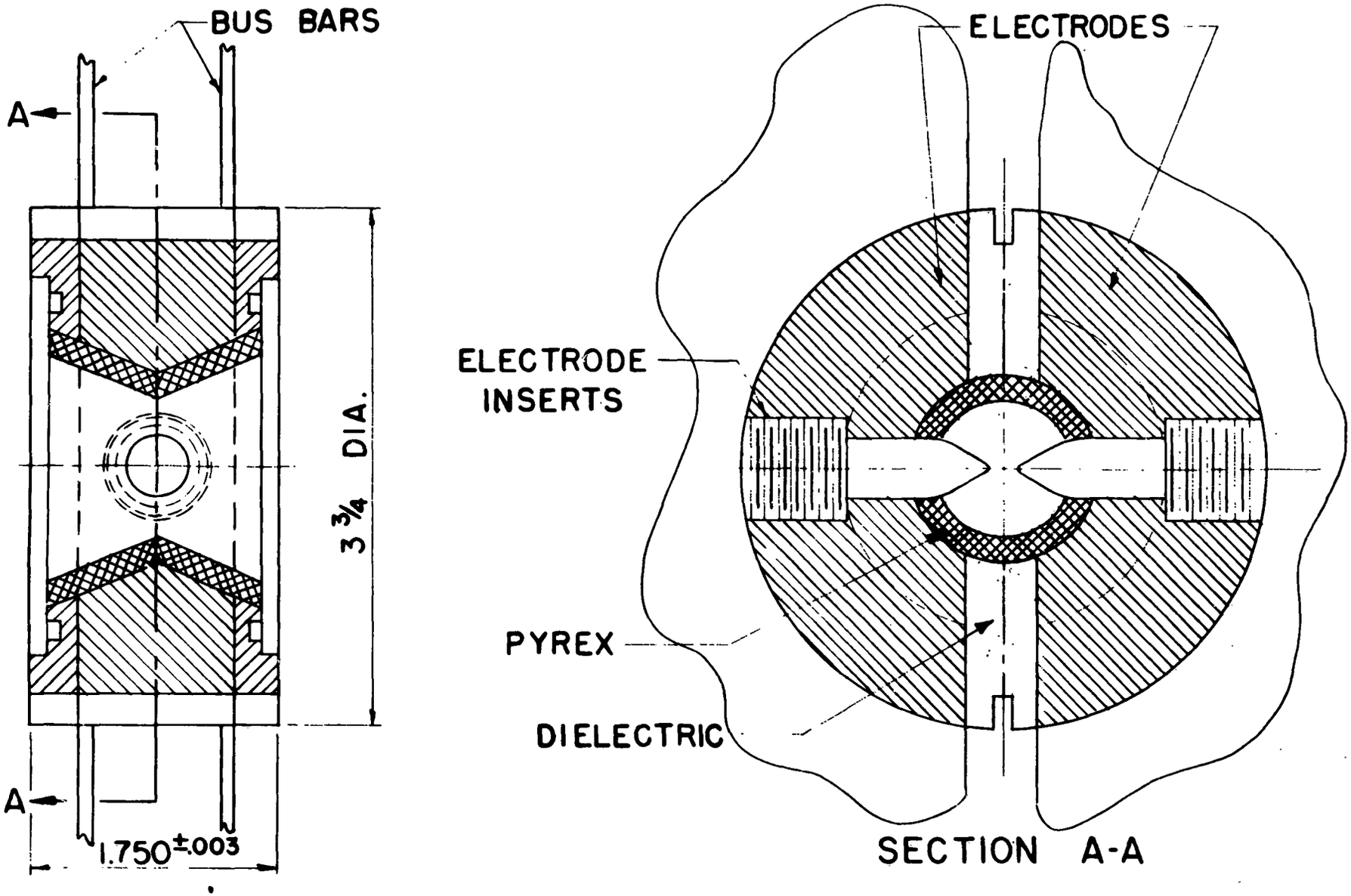

FIG. 5 BASIC DISCHARGE CARTRIDGE

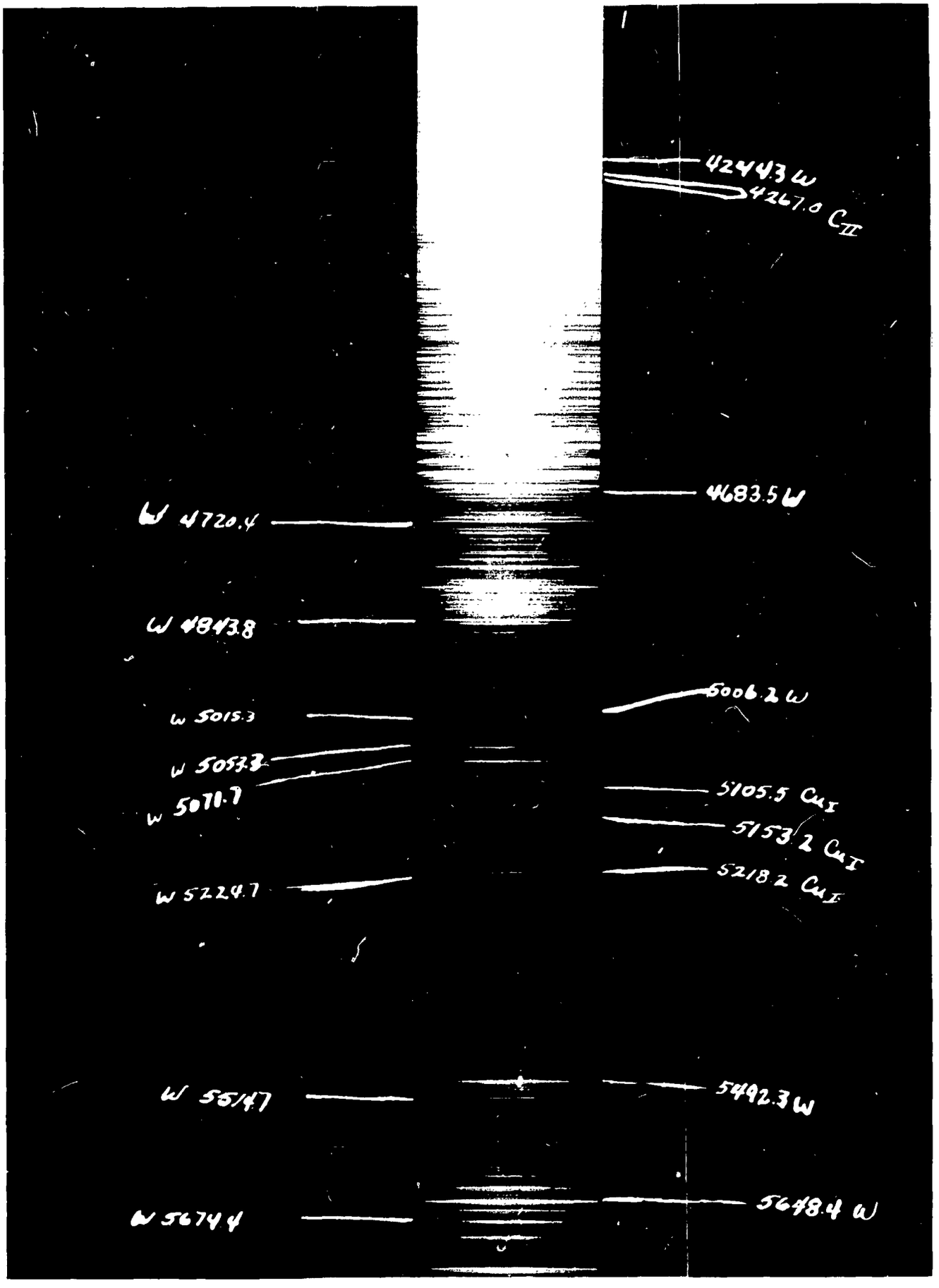
4244.3 W
4267.0 C II
4683.5 W
W 4720.4
W 4843.8
6006.2 W
W 5015.3
W 5057.3
W 5071.7
5105.5 Cu I
5153.2 Cu I
5218.2 Cu I
W 5224.7
W 5514.7
5492.3 W
W 5674.4
5648.4 W

Figure 6

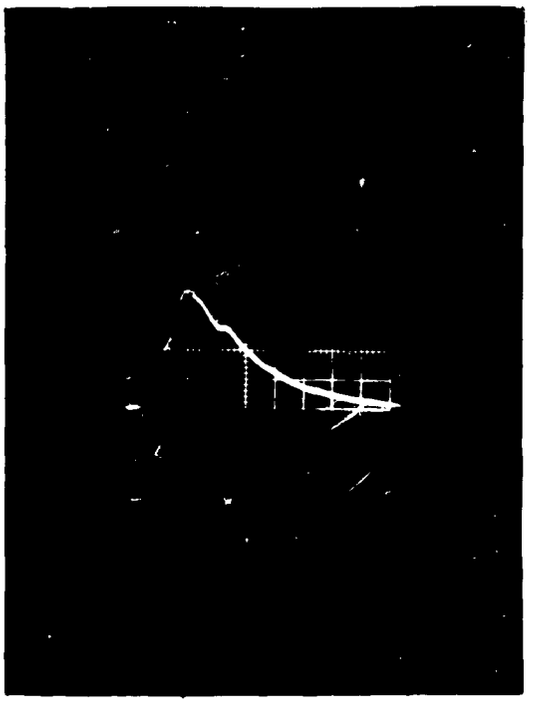

Figure 7 Oscilloscope Trace of Photocell Response

Horizontal deflection	2 μ sec/division
Vertical deflection	10 lumens/division

Discharge of 3000 joules in 2 mil wire

Figure 8a

Cracks in Pyrex

Energy Stored:
400 joules.
30 X Magnification.

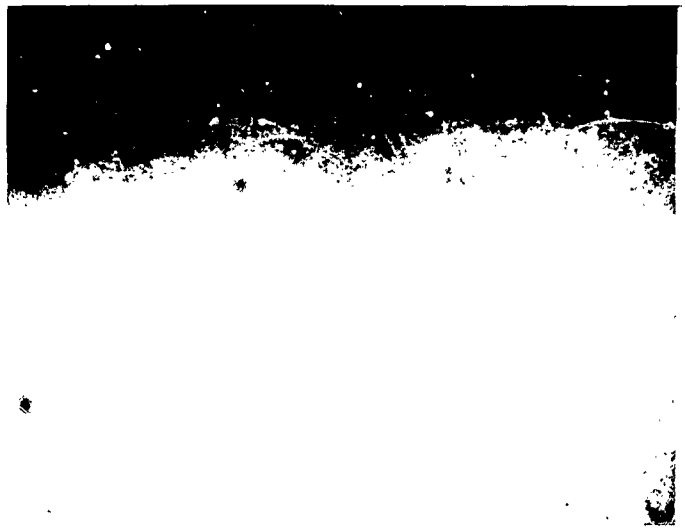

Figure 8b

Cracks in Pyrex

Energy Stored:
600 joules.
30 X Magnification.

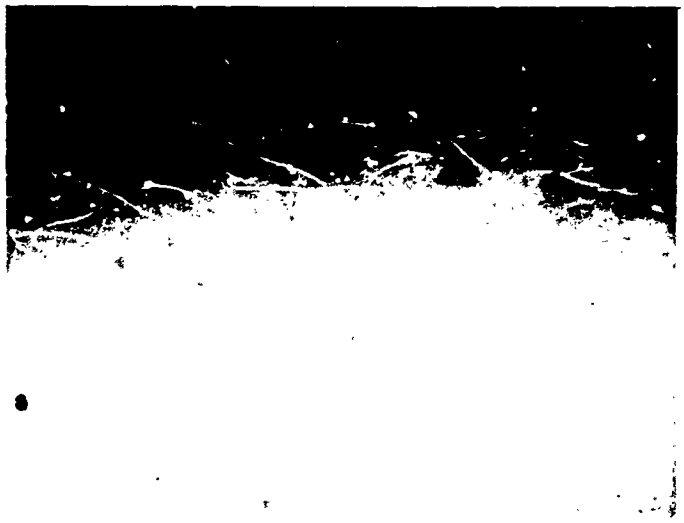

Figure 8c

Cracks in Pyrex

Energy Stored:
900 joules.
30 X Magnification.

Figure 9

Soda Lime Glass showing glass slivers sticking up out of the surface.

Energy Stored: 900 joules.

30 X Magnification.

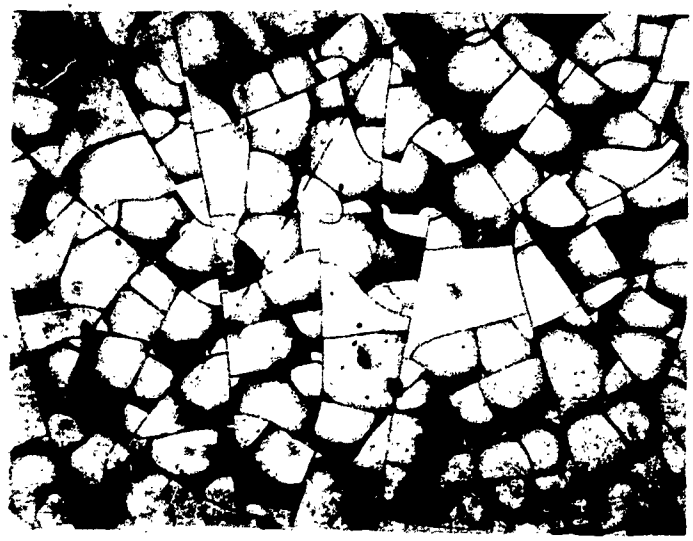

Figure 10 Photomicrograph of Bubbly Surface

Magnification - 82X

Sample at focus of ellipsoidal mirrors

Stored energy - 3000 joules

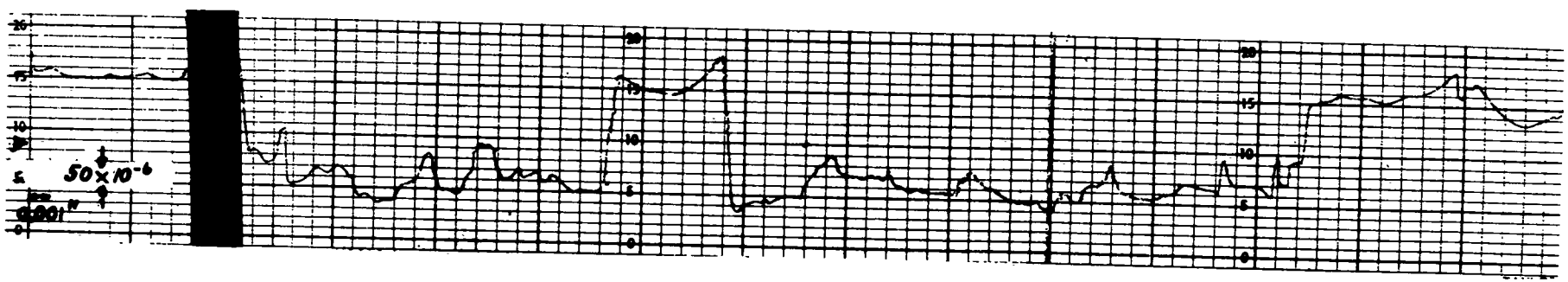

Figure 11. Profilometer Record of Surface

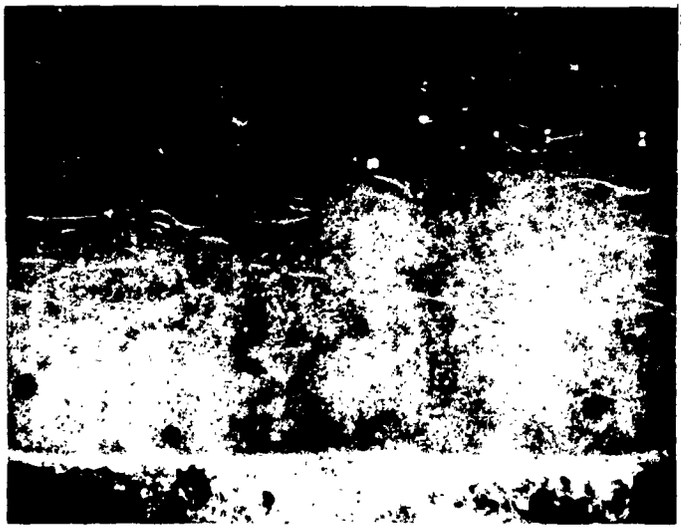

Figure 12

Cracks on Pyrex Glass showing the absence of cracks near a silver coating.

30 X Magnification.